Optica Applicata, Vol. XLI, No. 4, 2011

Relative intensity noise study in two mode quantum dot laser

ASHKAN HORRI[1*], SEYEDEH ZAHRA MIRMOEINI[1], RAHIM FAEZ[2]

[1]Department of Electrical Engineering, Arak Branch, Islamic Azad University, Arak, Iran

[2]Department of Electrical Engineering, Sharif University of Technology, Tehran, Iran

[*]Corresponding author: ashkan-hori.stu@iau-arak.ac.ir

In this paper, for the first time, we present a semiclassical noise model for InAs/GaAs quantum dot (QD) laser considering two photon modes, *i.e.*, ground and first excited states lasing. This model is based on the five level rate equations. By using this model, the effect of temperature variations on relative intensity noise (RIN) of QD laser is investigated. We find that the RIN significantly degrades when excited state (ES) lasing emerges at high temperature. Furthermore, we investigate the influence of the quantum dot numbers on the RIN properties.

Keywords: relative intensity noise, quantum dot laser, rate equations.

1. Introduction

Quantum dot (QD) lasers are important optical sources in optoelectronic communication systems. Low threshold current, wide frequency bandwidth, and low frequency chirp are advantages of these lasers [1, 2]. Intensity noise plays a destructive role in coherent optical communication systems. QD laser is a key component in these systems. Therefore, analysis of relative intensity noise (RIN) of QD lasers is very important. Theoretical analysis of intensity noise, in quantum cascade laser and single mode quantum dot laser, has already been reported [3, 4]. Recently, although many theoretical models for modulation response of two mode QD lasers have been described [5, 6], no studies have been made showing RIN characteristic of these lasers.

Noise behavior can be analyzed by introducing the Langevin noise terms into the rate equations. The five level rate equations, including two discrete electron energy levels and the level of wetting layer (WL) have been used to investigate the RIN of QD laser. The thermal carrier emission from excited state (ES) to the wetting layer and from the ground state (GS) to ES are added to the rate equations to demonstrate the influence of temperature on the RIN characteristics.

The paper is organized as follows. In Section 2, a semiclassical noise model for QD laser is introduced. In Section 3, a numerical results of RIN are presented. Finally, conclusion is presented in Section 4.

2. Semiclassical noise model

To determine the RIN of laser, we must obtain the spectral density of output power. For this purpose, first we add Langevin noise sources to the rate equations [6]:

$$\frac{\mathrm{d}n_0}{\mathrm{d}t} = \frac{n_1}{t_{10}}\left(1-\frac{n_0}{2N_d}\right) - \frac{n_0}{t_{sp}} - \frac{n_0}{t_{01}}\left(1-\frac{n_1}{4N_d}\right) - \frac{cg_0}{n_g}s_0\left(\frac{n_0}{N_d}-1\right) + F_{n0}(t) \tag{1}$$

$$\frac{\mathrm{d}n_1}{\mathrm{d}t} = \frac{n_w}{t_{w1}}\left(1-\frac{n_1}{4N_d}\right) + \frac{n_0}{t_{01}}\left(1-\frac{n_1}{4N_d}\right) - \frac{n_1}{t_{sp}} - \frac{n_1}{t_{10}}\left(1-\frac{n_0}{2N_d}\right) + \\ - \frac{n_1}{t_{1w}} - \frac{cg_1}{n_g}s_1\left(\frac{n_1}{2N_d}-1\right) + F_{n1}(t) \tag{2}$$

$$\frac{\mathrm{d}n_w}{\mathrm{d}t} = \frac{\eta I}{q} + \frac{n_1}{t_{1w}} - \frac{n_w}{t_{sp}} - \frac{n_w}{t_{w1}}\left(1-\frac{n_1}{4N_d}\right) + F_{nw}(t) \tag{3}$$

$$\frac{\mathrm{d}s_0}{\mathrm{d}t} = \frac{c}{n_g}\left[g_0\left(\frac{n_0}{N_d}-1\right)-\alpha\right]s_0 + \beta\frac{n_0}{t_{sp}} + F_{s0}(t) \tag{4}$$

$$\frac{\mathrm{d}s_1}{\mathrm{d}t} = \frac{c}{n_g}\left[g_1\left(\frac{n_1}{2N_d}-1\right)-\alpha\right]s_1 + \beta\frac{n_1}{t_{sp}} + F_{s1}(t) \tag{5}$$

where n_0, n_1, and n_w are the carrier numbers in the GS, ES, and the wetting layer, respectively; s_0 and s_1 denote the total photon population in GS and ES, respectively; g_0 and g_1 are the linear optical gains for GS and ES of QD laser. The associated time constants are carrier relaxation from wetting layer to ES (t_{w1}), carrier thermal escape from ES to the wetting layer (t_{1w}), carrier relaxation from ES to GS (t_{10}), carrier thermal escape from GS to ES (t_{01}), and spontaneous emission lifetime (t_{sp}). W and L are the width and length of laser cavity, n_g is the refractive index of the active region, α is the total loss, N_d is the total number of dots, and β is the spontaneous emission factor. $F_{n0}(t)$, $F_{n1}(t)$ and $F_{nw}(t)$ and are noise sources associated with carriers

in the GS, ES, and the wetting layer, respectively. $F_{s0}(t)$ and $F_{s1}(t)$ are noise sources for photons due to spontaneous emission. The thermal escape times are given by [6, 7]:

$$t_{01} = \frac{p_0}{p_1} t_{10} \exp\left(\frac{E_{10}}{k_B T}\right) \tag{6}$$

$$t_{1w} = \frac{p_1}{p_w} t_{w1} \exp\left(\frac{E_{w1}}{k_B T}\right) \tag{7}$$

where E_{10} and E_{w1} are transition energies from the ES to the GS and from wetting layer to the ES, respectively. P_0, P_1, and P_w represent the degeneracy of GS, ES, and wetting layer, respectively.

In the Markovian assumption, the Langevin noise sources satisfy [2, 3]:

$$\langle F_i(t) \rangle = 0 \tag{8}$$

$$\langle F_i(t) F_j(t) \rangle = 2D_{ij} \delta(t - t') \tag{9}$$

where angle brackets denote ensemble average and D_{ij} is the diffusion coefficient associated with the corresponding noise sources. The diffusion coefficient can be expressed as:

$$\langle F_{nw} F_{nw} \rangle = 2\left(\frac{n_{1dc}}{t_{1w}}\right) = 2D_{nwnw} \tag{10}$$

$$\langle F_{n1} F_{n1} \rangle = 2\left[\frac{n_{wdc}}{t_{w1}}\left(1 - \frac{n_{1dc}}{4N_d}\right) + \frac{n_{0dc}}{t_{01}}\left(1 - \frac{n_{1dc}}{4N_d}\right) + \frac{c g_1 s_{1dc}}{n_g}\right] = 2D_{n1n1} \tag{11}$$

$$\langle F_{n0} F_{n0} \rangle = 2\left[\frac{n_{1dc}}{t_{10}}\left(1 - \frac{n_{0dc}}{2N_d}\right) + \frac{c g_0 s_{0dc}}{n_g}\right] = 2D_{n0n0} \tag{12}$$

$$\langle F_{s1} F_{s1} \rangle = 2\left(\frac{c\alpha s_{1dc}}{n_g} + \frac{c g_1 s_{1dc}}{n_g}\right) = 2D_{s1s1} \tag{13}$$

$$\langle F_{s0} F_{s0} \rangle = 2\left(\frac{c\alpha s_{0dc}}{n_g} + \frac{c g_0 s_{0dc}}{n_g}\right) = 2D_{s0s0} \tag{14}$$

$$\langle F_{nw} F_{n1} \rangle = -\left[\frac{n_{wdc}}{t_{w1}} \left(1 - \frac{n_{1dc}}{4N_d} \right) + \frac{n_{1dc}}{t_{1w}} \right] = 2D_{nwn1} \tag{15}$$

$$\langle F_{n1} F_{n0} \rangle = -\left[\frac{n_{0dc}}{t_{01}} \left(1 - \frac{n_{1dc}}{4N_d} \right) + \frac{n_{1dc}}{t_{10}} \left(1 - \frac{n_{0dc}}{2N_d} \right) \right] = 2D_{n1n0} \tag{16}$$

$$\langle F_{n1} F_{s1} \rangle = -\left[\frac{cg_1}{n_g} \left(1 + \frac{n_{1dc}}{N_d} \right) + \frac{\beta n_{1dc}}{t_{sp}} \right] = 2D_{n1s1} \tag{17}$$

$$\langle F_{n0} F_{s0} \rangle = -\left[\frac{cg_0}{n_g} \left(1 + \frac{n_{0dc}}{N_d} \right) + \frac{\beta n_{0dc}}{t_{sp}} \right] = 2D_{n0s0} \tag{18}$$

$$\begin{aligned} \langle F_{n1} F_{s0} \rangle &= \langle F_{n0} F_{s1} \rangle = \langle F_{nw} F_{s0} \rangle = \langle F_{nw} F_{s1} \rangle = \\ &= \langle F_{s0} F_{s1} \rangle = \langle F_{nw} F_{n0} \rangle = 0 \end{aligned} \tag{19}$$

where n_{0dc}, n_{1dc}, n_{wdc}, s_{0dc}, and s_{1dc} are the average values obtained from the steady state solution of Eqs. (1)–(5). The total photon number S_T is obtained by adding photon numbers in the cavity with ES and GS resonant energies.

With small signal analysis of the rate Eqs. (1)–(5), and using the Fourier transform, we obtain the following linear algebraic equations

$$\begin{bmatrix} a_1 & a_2 & a_3 & a_4 & a_5 \\ a_6 & a_7 & a_8 & a_9 & a_{10} \\ a_{11} & a_{12} & a_{13} & a_{14} & a_{15} \\ a_{16} & a_{17} & a_{18} & a_{19} & a_{20} \\ a_{21} & a_{22} & a_{23} & a_{24} & a_{25} \end{bmatrix} \begin{bmatrix} \Delta n_0(w) \\ \Delta n_1(w) \\ \Delta n_w(w) \\ \Delta s_0(w) \\ \Delta s_1(w) \end{bmatrix} = \begin{bmatrix} F_{n0}(w) \\ F_{n1}(w) \\ F_{nw}(w) \\ F_{s0}(w) \\ F_{s1}(w) \end{bmatrix} \tag{20}$$

where $\Delta n_0(w)$, $\Delta n_1(w)$, and $\Delta n_w(w)$ are the carrier fluctuations in GS, ES and the wetting layer, respectively. $\Delta s_0(w)$ and $\Delta s_1(w)$ are the photon fluctuations in GS and ES, respectively. The above matrix elements, are given by:

$$a_2 = -\left(\frac{1}{t_{tw}} + \frac{n_{wdc}}{4N_d t_{w1}} \right) \tag{21a}$$

$$a_3 = \frac{1}{t_{sp}} + \frac{1}{t_{w1}} \left(1 - \frac{n_{1dc}}{4N_d} \right) + jw \tag{21b}$$

$$a_6 = \frac{n_{1dc}}{2N_d t_{10}} + \frac{1}{t_{sp}} + \frac{1}{t_{01}}\left(1 - \frac{n_{1dc}}{4N_d}\right) + \frac{cg_0 s_{0dc}}{n_g N_d} + jw \tag{21c}$$

$$a_7 = -\left[\frac{1}{t_{10}}\left(1 - \frac{n_{0dc}}{2N_d}\right) + \frac{n_{0dc}}{4N_d t_{01}}\right] \tag{21d}$$

$$a_9 = \frac{cg_0}{n_g}\left(\frac{n_{0dc}}{N_d} - 1\right) \tag{21e}$$

$$a_{11} = -\left[\frac{1}{t_{01}}\left(1 - \frac{n_{1dc}}{4N_d}\right) + \frac{n_{1dc}}{2N_d t_{10}}\right] \tag{21f}$$

$$a_{12} = \frac{n_{wdc}}{4N_d t_{w1}} + \frac{n_{0dc}}{4N_d t_{01}} + \frac{1}{t_{sp}} + \frac{1}{t_{10}}\left(1 - \frac{n_{0dc}}{2N_d}\right) + \frac{1}{t_{1w}} + \\ + \frac{cg_1 s_{1dc}}{n_g N_d} + jw \tag{21g}$$

$$a_{13} = -\frac{1}{t_{w1}}\left(1 - \frac{n_{1dc}}{4N_d}\right) \tag{21h}$$

$$a_{15} = \frac{cg_1}{n_g}\left(\frac{n_{1dc}}{N_d} - 1\right) \tag{21i}$$

$$a_{16} = -\left(\frac{cg_0 s_{0dc}}{n_g N_d} + \frac{\beta}{t_{sp}}\right) \tag{21j}$$

$$a_{19} = -\left[\frac{cg_0}{n_g}\left(\frac{n_{0dc}}{N_d} - 1\right) - \frac{c\alpha}{n_g} - jw\right] \tag{21k}$$

$$a_{22} = -\left(\frac{cg_1 s_{1dc}}{n_g N_d} + \frac{\beta}{t_{sp}}\right) \tag{21l}$$

$$a_{25} = -\left[\frac{cg_1}{n_g}\left(\frac{n_{1dc}}{N_d} - 1\right) - \frac{c\alpha}{n_g} - jw\right] \tag{21m}$$

$$a_1 = a_4 = a_5 = a_8 = a_{10} = a_{14} = a_{17} = a_{18} = \\ = a_{20} = a_{21} = a_{23} = a_{24} = 0 \tag{21n}$$

Solving Eq. (20) with respect to the total photon fluctuation Δs_T, one can write:

$$\Delta s_T = \frac{1}{H(w)}\left[r_{n0}(w)F_{n0} + r_{n1}(w)F_{n1} + r_{nw}(w)F_{nw} + r_{s0}(w)F_{s0} + r_{s1}(w)F_{s1}\right] \tag{22}$$

where

$$r_{n0}(w) = a_{16}a_2a_{13}a_{25} + a_{16}a_{22}a_3a_{15} + a_{11}a_{22}a_3a_{19} - a_{16}a_{12}a_3a_{25} \tag{23a}$$

$$r_{n1}(w) = a_{16}a_7a_3a_{25} + a_{16}a_{22}a_3a_9 - a_6a_{22}a_3a_{19} \tag{23b}$$

$$r_{nw}(w) = a_6a_{22}a_{13}a_{19} - a_{16}a_{22}a_{13}a_9 - a_{16}a_7a_{13}a_{25} \tag{23c}$$

$$r_{s0}(w) = a_6a_{12}a_3a_{25} - a_6a_2a_{13}a_{25} - a_6a_{22}a_3a_{15} + \\ - a_{11}a_7a_3a_{25} - a_{11}a_{22}a_3a_9 \tag{23d}$$

$$r_{s1}(w) = a_6a_{12}a_3a_{19} + a_{16}a_2a_{13}a_9 - a_{16}a_7a_3a_{15} - a_6a_2a_{13}a_{19} + \\ - a_{11}a_7a_3a_{19} - a_{16}a_{12}a_3a_9 \tag{23e}$$

$$H(w) = a_6a_{12}a_3a_{19}a_{25} + a_{16}a_2a_{13}a_9a_{25} - a_6a_2a_{13}a_{19}a_{25} - a_6a_{22}a_3a_{15}a_9 + \\ - a_{11}a_7a_3a_{19}a_{25} - a_{16}a_{12}a_3a_9a_{25} \tag{23f}$$

The total relative intensity noise (RIN) is defined as:

$$\frac{\mathrm{RIN}(w_0)}{\Delta f} = \frac{2S_p(w_0)}{(S_{Tdc})^2} \tag{24}$$

where $S_p(w_0)$ is the spectral density at a frequency w_0, S_{Tdc} is the total photon number, and Δf is the bandwidth of spectrum analyzer filter.

The spectral density is given by [2, 3]:

$$S_p(w) = \lim_{T\to\infty}\frac{1}{T}\left|\Delta S_T(w)\right| \tag{25}$$

where

$$\lim_{T\to\infty}\frac{1}{T}\left[F_i(w)\,F_j^*(w)\right] = \langle F_i\,F_j\rangle = 2D_{ij} \tag{26}$$

The RIN is given by using Eqs. (22)–(26):

$$\frac{\mathrm{RIN}}{\Delta f} = \frac{2}{S_{Tdc}^2|H(w)|^2}\left[2D_{nwnw}|r_{nw}(w)|^2 + 2D_{n1n1}|r_{n1}(w)|^2 + \right.$$

$$\left. + 2D_{n0n0}|r_{n0}(w)|^2 + 2D_{s0s0}|r_{s0}(w)|^2 + 2D_{s1s1}|r_{s1}(w)|^2 + \right.$$

$$+ 4D_{nwn1}\mathrm{Re}(r_{nw}\, r_{n1}) + 4D_{n1n0}\mathrm{Re}(r_{n1}\, r_{n0}) + 4D_{n1s1}\mathrm{Re}(r_{n1}\, r_{s1}) +$$
$$+ 4D_{n0s0}\mathrm{Re}(r_{ns0}\, r_{s0})\Big] \tag{27}$$

where Re(...) denotes real part of a complex number.

3. Results

In this section, we analyze the RIN of QD laser. The QD laser used in our simulation is grown by molecular beam epitaxy. The active region is formed by five layers of InAs QDs, which are covered by a 4 nm $In_{0.17}Ga_{0.83}As$ strain reducing layer and separated from each other by a 40 nm GaAs spacer layer. The areal dot density is 25×10^{10} cm^{-2}. The laser cavity is covered by 1.4 μm of $Al_{0.4}Ga_{0.6}As$ which is *n*-type on the substrate side and *p*-doped on the top side. The cavity length is 1000 μm while its width is 4 μm. The facets were coated with reflectivity of 60% and 95%, respectively. The values of the parameters used in numerical calculation, are listed in the Table.

Figure 1 shows the calculated output photon numbers for the GS and ES as a function of injected current at 50 °C. As shown in Fig. 1, the GS threshold current is 15 mA and once the second lasing of the ES appears at about 70 mA, the emission of the GS saturates completely and the ES emission increases linearly. This result is in agreement with measured result reported by PENG-FEI XU *et al*. [6].

T a b l e. QD laser parameter values [5, 6].

Symbol	Description	Value
N_d	Areal dot density	25×10^{10} cm^{-2}
g_0	GS saturation gain	20 cm^{-1}
g_1	ES saturation gain	40 cm^{-1}
t_{sp}	Spontaneous emission lifetime	1 ns
W	Cavity width	4 μm
L	Cavity length	1000 μm
η	Carrier injection efficiency	0.6
α	Total loss of cavity	540 cm^{-1}
β	Spontaneous emission factor	10^{-5}
n_g	Refractive index	3.6
c	Speed of light	3×10^8 m/s
t_{w1}	Carrier relaxation lifetime from WL to ES	1 ps
t_{10}	Carrier relaxation lifetime from ES to GS	2 ps
q	Electron charge	1.6×10^{-19} C
k_B	Boltzmann constant	8.617×10^{-5} eV/K
P_0	Degeneracy of the GS	2
P_1	Degeneracy of the ES	4
E_{10}	Transition energy of electrons from ES to GS	46 meV
E_{w1}	Transition energy of electrons from WL to ES	200 meV

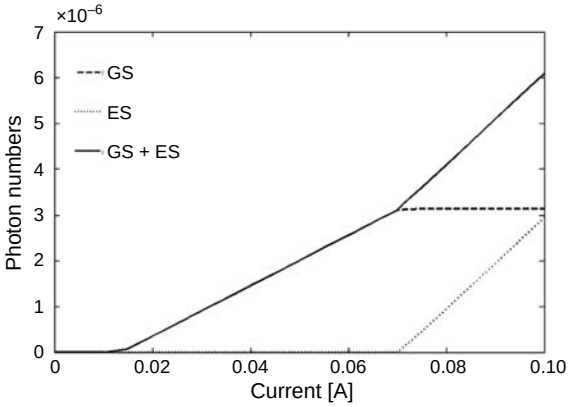

Fig. 1. Calculated photon numbers in the cavity as a function of injected current.

Before the bias current of 70 mA, the laser emission wavelength is 1.307 μm corresponding to the GS lasing. When increasing the bias current to 70 mA, two different emission wavelengths of 1.233 μm (ES) and 1.304 μm (GS) exist simultaneously with the energy separation between the two states of 55 meV.

Figure 2**a**, shows the calculated RIN under different injected current at 20 °C. It can be found that the increase of bias current from 50 to 90 mA leads to the lower RIN.

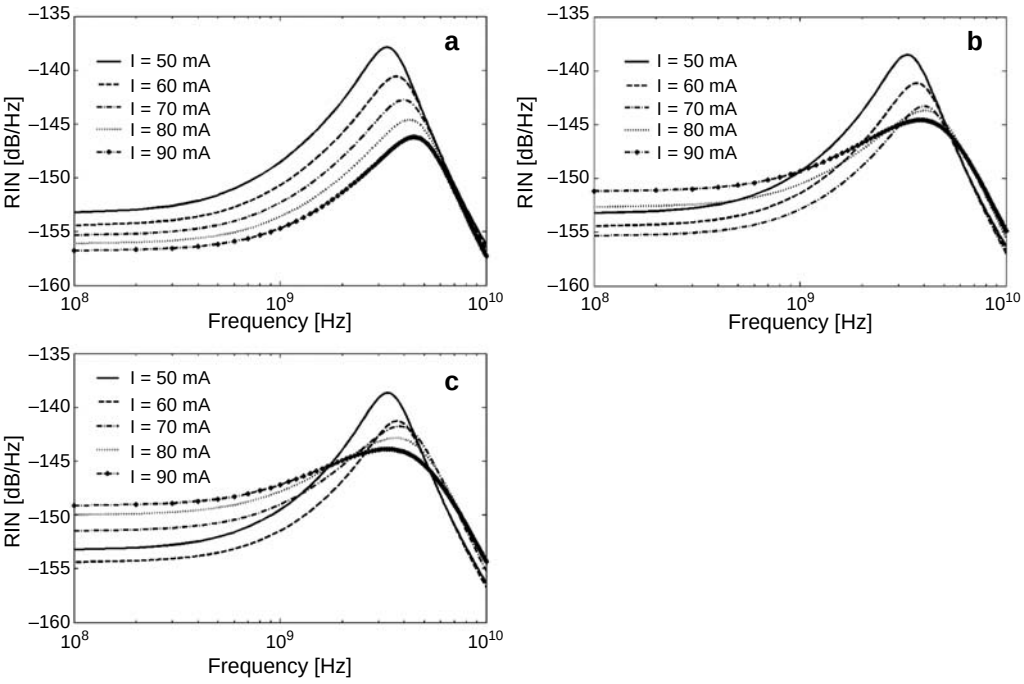

Fig. 2. Calculated RIN as a function of frequency for different injected current at T = 20 °C (**a**), T = 50 °C (**b**), and T = 60 °C (**c**).

Also, with an increase of the injected current, the resonance peak shifts to higher frequency. Figure 2**b** shows the calculated RIN at 50 °C, when the bias current increases from 50 to 90 mA. As shown in Fig. 2**b**, when the bias current is under 70 mA, the RIN shows the same rule as that at 20 °C, but for the bias current of 80 mA and 90 mA, the RIN significantly degrades, especially at low frequencies. In Figure 2**c**, the bias current for this significant degradation in the RIN decreases to 70 mA.

Figure 3 shows the variation of average value of RIN with injected current at different temperatures. It shows that, at a temperature of 50 °C, as the injected current increases from 70 to 120 mA, the RIN first slightly degrades and then goes down slowly. At a temperature of 60 °C, the bias current for this degradation in the RIN decreases to 60 mA. At a temperature of 20 °C, the condition for population inversion of ES cannot be satisfied even at the injected current of 120 mA. We can find that, as the injected current increases at first, the optical power increases, and therefore the RIN is enhanced. But when the ES lasing occurs, the limited relaxation time from the ES to the GS degrades the RIN. Therefore, theoretical analysis demonstrates that ES lasing can degrade the RIN of QD laser at elevated temperature.

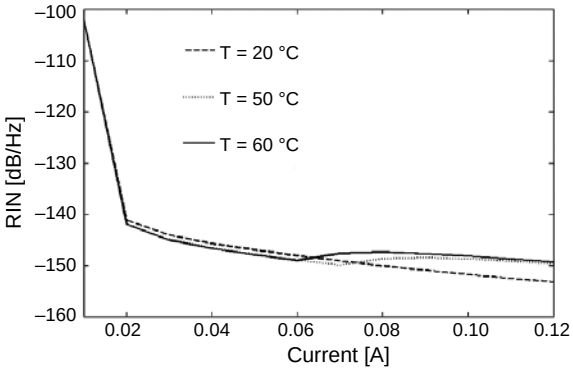

Fig. 3. Variation of average value of RIN in the frequency range 0.1–10 GHz versus current, for different temperatures.

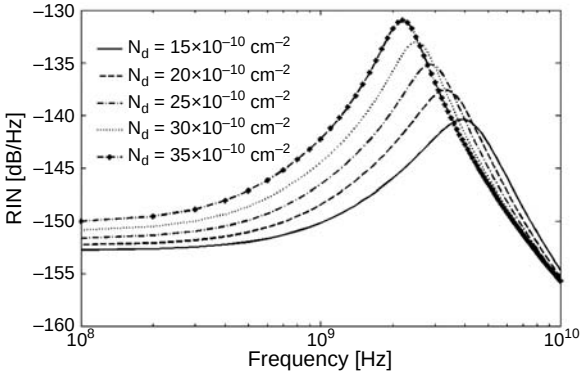

Fig. 4. Calculated RIN as a function of frequency for different QD densities at T = 50 °C.

To eliminate this problem, doping QDs with acceptors are proposed. Owing to the larger separation of electron levels in QDs, the injected electrons lie mostly in their ground states. The large hole occupancy built in by the *p*-doping ensures that injected electrons always find ground state holes to recombine.

Figure 4, shows the RIN as a function of frequency for different QD numbers. As shown in the figure, the RIN is enhanced for lower QD numbers. Indeed, decreasing QD numbers leads to a higher occupation probability, which results in higher output power, and consequently, enhancement of the RIN.

4. Conclusions

We have presented a semiclassical model for intensity noise of two mode InAs/GaAs QD laser based on the five level rate equations. We have found that ES lasing can degrade the RIN of QD lasers at elevated temperature. Also, we found that decreasing the QD numbers leads to a lower RIN.

References

[1] SUGAWARA M., *Self Assembled InGaAs/GaAs Quantum Dot*, 1th Edition, Academic Press, San Diego, 1999, pp. 83–97.

[2] COLDREN L.A., CORZINE S.W., *Diode Laser and Photonic Integrated Circuit*, 1th Edition, Wiley--Interscience, New York, 1995, pp. 220–240.

[3] GENSTY T., ELSÄßER W., *Semiclassical model for the relative intensity noise of intersubband quantum cascade lasers*, Optics Communications **256**(1–3), 2005, pp. 171–183.

[4] AL-KHURSAN A.H., *Intensity noise characteristics in quantum dot lasers: Four-level rate equations analysis*, Journal of Luminescence **113**(1–2), 2005, pp. 129–136.

[5] O'DRISCOLL I., HUTCHINGS M., SMOWTON P.M., BLOOD P., *Many-body effects in InAs/GaAs quantum dot laser structures*, Applied Physics Letters **97**(14), 2010, p. 141102.

[6] PENG-FEI XU, TAO YANG, HAI-MING JI, YU-LIAN CAO, YONG-XIAN GU, YU LIU, WEN-QUAN MA, ZHAN-GUO WANG, *Temperature-dependent modulation characteristics for 1.3 μm InAs/GaAs quantum dot lasers*, Journal of Applied Physics **107**(1), 2010, p. 013102.

[7] TONG C.Z., YOON S.F., NGO C.Y., LIU C.Y., LOKE W.K., *Rate equations for 1.3 μm dots-under-a-well and dots-in-a-well self-assembled InAs–GaAs quantum dot lasers*, IEEE Journal of Quantum Electronics **42**(11), 2006, pp. 1175–1183.

Received December 23, 2010
in revised form March 20, 2011